Astronomy
&
Astrophysics

Age and metallicity of a globular cluster in the dwarf spheroidal galaxy DDO 78

M. E. Sharina[1,3], O. K. Sil'chenko[2,4], and A. N. Burenkov[1,3]

[1] Special Astrophysical Observatory, Russian Academy of Sciences, N.Arkhyz, KChR, 369167, Russia
[2] Sternberg Astronomical Institute, Universitetskij Prospect 13, 119992 Moscow, Russia
[3] Isaac Newton Institute, Chile, SAO Branch
[4] Isaac Newton Institute, Chile, Moscow Branch

Abstract. We present the results of moderate resolution spectroscopy for a globular cluster in the M81 group dwarf spheroidal galaxy DDO 78. The DDO 78 globular cluster, 4 Milky Way globular clusters, spectroscopic and radial velocity standards were observed with the Long-slit spectrograph of the 6-m telescope (SAO RAS, Russia). Lick spectrophotometric indices were determined in the bandpasses adopted by Burstein et al. (1984). We have derived the mean metallicity of the globular cluster in DDO78 to be [Fe/H] = -1.6 ± 0.1 dex by taking the weighted mean of metallicities obtained from the strength of several absorption features. We have estimated an age for the globular cluster of 9–12 Gyr similar to that found for the Galactic globular cluster NGC 362, which resembles the DDO 78 cluster in its chemical abundance and integrated spectrophotometric properties.

Key words. galaxies: dwarf – galaxies: star clusters – galaxies: individual: DDO 78

1. Introduction

The dominant type of dwarf galaxy in the local Universe is the dwarf spheroidal galaxy (DSph). These systems are characterized by low luminosities ($M_V > -14$), low stellar density ($\mu_v(0) \gtrsim 22^{\mathrm{m}}/\square''$), small spatial extent (core radii <a few hundred parsecs), HI masses $M_{\mathrm{HI}} \lesssim 10^5\ M_\odot$ and a lack of current star formation (Grebel 2000; Stetson et al. 1998). New deep C-M diagrams and spectroscopy of individual red giants in several Local Group dSphs have shown us that, in spite of their current quiescent appearance, most of the systems have had surprisingly complicated evolutionary histories (Harbeck et al. 2002). It would be interesting to compare the chemical and star formation histories for DSphs in the Local group and in the other nearby groups. It is a difficult task, because the observational magnitude limit does not allow us to observe the HB stars in the galaxies at a distance of >3 Mpc. Globular clusters (GCs) found in some DSphs are ideal probes of chemical histories and evolution of their host galaxies. They are bright enough to be observed at large distances. If the correlations between key spectral indices, metallicities and ages are common for GCs in all types of galaxies, we can determine the age for the given particular GC by using the evolutionary population synthesis models (e.g. Worthey 1994) and can compare our results with the data available in the literature on the Milky Way globular clusters.

The group of galaxies around the bright spiral M 81 is one of the nearest prominent groups in the vicinity of the Local Group. It is situated at a distance of ~3.7 Mpc and consists of at least 12 DSphs and 12 dwarf irregular galaxies (Karachentsev et al. 2002). DDO 78 is one of the faintest DSphs of the group ($M_V = -12.83$). According to Karachentseva et al. (1987), DDO 78 has a very flat surface brightness profile with $\mu_{B(0)} = 25.1^{\mathrm{m}}/\square''$, $r_{\mathrm{ef}} = 32''$, and $B(t) = 15.8$. It was not detected in HI by Fisher & Tully (1981) and van Driel et al. (1998). An accurate distance modulus of DDO 78 is $(m - M)_0 = 27.85 \pm 0.15$ according to Karachentsev et al. (2000). These authors found globular cluster candidates in five dwarf spheroidal galaxies of the M 81 group and measured their basic photometric parameters. The brightest globular cluster candidate in the DSph galaxy DDO 78 has the integrated apparent magnitude $V_t = 19.45$, the integrated color after correction for Galactic reddening $(V - I)_0 = 1.07$, the angular half-light radius $R(0.5L) = 0.3''$, the central surface brightness $\mu_v(0) = 18.0^{\mathrm{m}}/\square''$, the linear projected separation of the globular cluster from the galaxy center of 0.26 kpc. Sharina et al. (2001) measured a heliocentric radial velocity of the globular cluster candidate in DDO 78 to be 55 $\pm$ 10 km s^{-1} by cross-correlation with template stars and established the object as a bona fide member of the galaxy. The present work continues our study of the dwarf spheroidal galaxies in the M 81 group. The spectra of the globular cluster in DDO 78 (Fig. 1) are of rather high signal-to-noise ratio and are suitable for quantitative spectrophotometric study.

2. Observations and data reduction

The observations were performed with the Long-slit spectrograph UAGS (Afanasiev et al. 1995) at the prime focus

Table 1. Observational log.

Object	Date	Exposure	Seeing
Globular cluster	18.01.2001	2×1200 s	1″3
in DDO 78	18.01.2001	2×2400	
	19.01.2001	8×1200	1.3
NGC 2419	19.01.2001	2×600	1.3
NGC 4147	19.01.2001	2×600	1.3
Pal1	22.01.2001	3×900	2.2
NGC 5272	22.01.2001	3×600	2.2
BF 10078 (F8 V)	18.01.2001	3×10	1.3
BF 11123 (G8 V)	18.01.2001	3×30	1.3
BF 13987 (F8 VI)	18.01.2001	3×60	1.3
BF 18804 (G9 V)	19.01.2001	2×20	1.3
BF 18757 (G9 V)	19.01.2001	2×10	1.3
BF 15344 (F8 V)	22.01.2001	2×20	2.2
BF 16879 (G8 IV)	22.01.2001	2×20	2.2
HD 073593 (G8IV)	18.04.2002	2×5	4.0
HD 091739 (G0)	18.04.2002	2×40	4.0
HD 152792 (G0V)	18.04.2002	2, 5	4.0
HD 142373 (F8Ve)	18.04.2002	2×1	4.0
BD 28 4211	18.01.2001	2×90	1.3
	19.01.2001	2×150	1.3
Feige 34	22.01.2001	2×120	2.2
HZ 44	18.04.2002	240, 120	4.0

Table 2. Additional observational data on the Milky Way globular clusters.

Object	RA (2000.0)	Dec	PA of the slit	Aperture along the slit
NGC 2419	07 38 08.22	+38 52 56.42	152°6	14″
NGC 4147	12 10 06.66	+18 32 34.31	102.6	20
Pal 1	03 33 20.85	+79 34 57.33	151.2	7
NGC 5272	13 42 11.56	+28 22 32.60	51.8	60

Table 3. Measured heliocentric radial velocities of the globular clusters in comparison with corresponding data from Harris (1996).

Object	V_h (our), km s^{-1}	V_h (Harris), km s^{-1}
GG in DDO 78	55 ± 10	–
NGC 4147	189 ± 11	183.2
NGC 2419	-4.4 ± 23	-20.0
NGC 5272	-130 ± 15	-148.5
Pal 1	-60 ± 25	-82.8
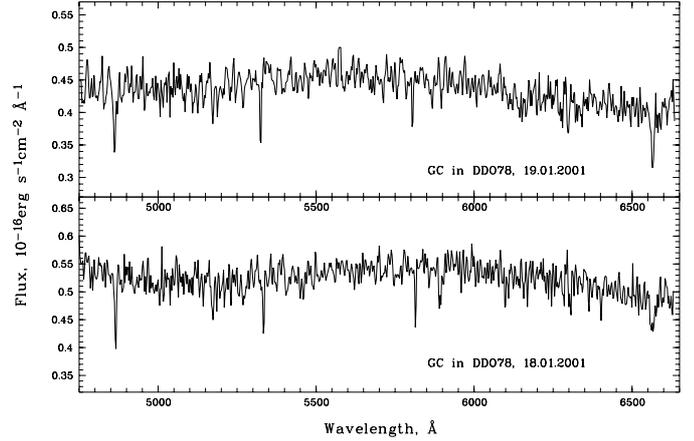
Fig. 1. Two spectra of the globular cluster in DDO 78 obtained on 18.01.2001 (top) and on 19.01.2001 (bottom).
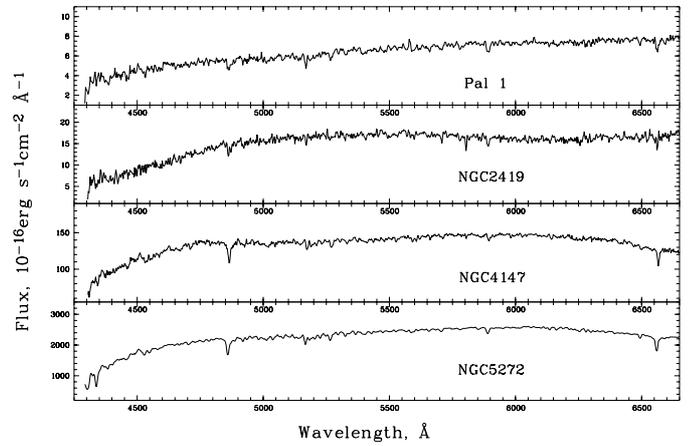
Fig. 2. Spectra of Galactic globular clusters NGC 5272, NGC 2419, NGC 4147 and Pal 1 observed by us.

of the 6-m telescope (SAO RAS, Russia) during 4 nights in January 2001 at a seeing of ~1″ (see Table 1 for details). An additional observation of stars from the Lick/IDS sample of Worthey et al. (1994) was performed in April 2002. The long-slit 130″ spectra were obtained with a CCD-detector having 1024×1024 pixels with a 24×24 μm pixel size. For all observations we used a grating of 651 grooves/mm with a corresponding dispersion of 2.4 Å/pixel and a spectral resolution of 7–9 Å. The slit positions were chosen to cross the star cluster. The wavelength range was 4500–6900 Å. In all the cases the slit width was 2″. The scale along the slit was 0.41″/pixel. The reference spectra of an Ar-Ne-He lamp were exposed before and after each observation to provide wavelength calibration. For velocity calibration we obtained long-slit spectra of seven radial-velocity standard stars (Barbier-Brossat & Figon 2000) (see Table 1). The spectrophotometric standard stars BD 28 4211, HZ 44 and Feige 34 (Bohlin 1996) were observed for flux calibration.

The data reduction was performed using the LONG package in MIDAS. The subsequent data analysis was also carried out in MIDAS. The primary data reduction included cosmic-ray removal, bias subtraction and flat-field correction. After wavelength calibration and sky subtraction, the spectra

were corrected for atmospheric extinction and flux-calibrated. Then rows of every linearized two-dimensional spectrum were summed in the spatial direction to yield a final one-dimensional spectrum. All individual exposures of the same object observed at the same night were then co-added to increase the S/N ratio.

In order to obtain integrated spectra for the Milky Way clusters (Fig. 2), we averaged the spectra of different zones and individual stars in the core of each cluster. The sizes of the integrated apertures along the slit, equatorial coordinates of the GC centers and positional angles of the slit are listed in Table 2. All the spectra of the given particular GC were recorded at the same slit position across the center of the object.

Radial velocities of the globular clusters were obtained by cross-correlation with template stars and were used for a subsequent abundance analysis. A comparison of the radial velocities measured by us with the corresponding values from Harris (1996) (Table 3, this paper) shows a good agreement.

3. Measurement of spectral indices and errors

Absorption-line indices were measured for each object according the index definitions reported by Burstein et al. (1984). Each line index is a measurement of the flux contained in the wavelength region centered on the feature relative to that contained in the red and blue "continuum" regions close to the features (Faber et al. 1977). We computed the index I as:

$$I = -2.5 \log \frac{F_I}{F_{C1} + k\,(F_{C2} - F_{C1})},$$

where F_I is the mean flux in the feature, and F_{C1}, F_{C2} are the mean fluxes in the continuum bandpasses. k is a constant defined by interpolation between the central wavelengths in the blue and red bandpasses with respect to the central wavelength of the bandpass centered on the feature:

$$k = \frac{\left(\lambda_{F_{I_2}} - \lambda_{F_{C1_2}}\right) + \left(\lambda_{F_{I_1}} - \lambda_{F_{C1_1}}\right)}{\left(\lambda_{F_{C2_2}} - \lambda_{F_{C1_2}}\right) + \left(\lambda_{F_{C2_1}} - \lambda_{F_{C1_1}}\right)}.$$

It is possible to convert the index values from the magnitudes to pseudo-equivalent widths and vice versa by the formulae:

$$EW(I) = (\lambda_2 - \lambda_1)\left(1 - 10^{-\frac{I}{2.5}}\right)$$

$$I(EW) = -2.5 \log\left(1 - \frac{EW}{\lambda_2 - \lambda_1}\right).$$

We have derived the errors of the measurements of the line indices according to equations of Cardiel et al. (1998). The most common sources of systematic errors in the measurement of line-strength indices are: flux calibration effects, spectral resolution, sky subtraction uncertainties, scatter light effects, wavelength calibration and radial velocity errors, seeing and focus corrections, response deviations from linearity and random Poisson noise. We used a correlation between the measured absolute index error and the mean $(S/N\text{-ratio})/\text{Å}$ studied by Cardiel et al. (1998) to derive the error of our line-strength index measurements. We computed the mean signal-to-noise

ratio in each bandpass via the sum of the individual S/N ratios in each pixel:

$$SN(\text{Å}) = \frac{1}{N\sqrt{\theta}}\sum_{i=1}^{N}\frac{S(\lambda_i)}{\sigma(\lambda_i)},$$

where θ is the dispersion (in Å/pixel).

Two spectra of the globular cluster in DDO 78 were obtained during two nights under similar observational conditions (Table 1, Fig. 1). The final index values for the GC in DDO 78 (Table 5) are a weighted average of the indices from the two spectra using $\frac{1}{\sigma_i^2}$ as a weight. The final index photon errors, σ_I, are given by the reduced photon error:

$$\sigma_I = \left(\sum_{i=1}^{N}\frac{1}{\sigma_i^2}\right)^{-1/2}.$$

To check the calibration of our index measurements into the standard Lick system, we observed 4 stars from the list of Worthey et al. (1994). A comparison of the measured long-slit indices with those from Worthey et al. (1994) is given in Table 4 together with the measured indices of the twilight sky. The Lick indices of the twilight sky are known from the extensive observations with the Multi-Pupil Fiber Spectrograph of the 6 m telescope that are well calibrated in the standard Lick system through careful monitoring of the standard stars (the last and most complete calibration of the MPFS index system into the standard Lick one can be found in Afanasiev & Sil'chenko 2002). One can see that our index system coincides with the standard Lick one within the errors of measurements. Besides the stars, we observed also the cores of 4 galactic clusters NGC 5272, NGC 2419, NGC 4147 and Pal 1 to compare them with the GC in DDO 78. The candidates for observations were chosen to conform to an expected metallicity of the globular cluster in DDO 78. The measured indices in the Lick system for the globular clusters are listed in Table 5.

To investigate the properties of the GC in DDO 78 we supplemented our data by observations of Cohen et al. (1998), Covino et al. (1995), Burstein et al. (1984), and Brodie & Huchra (1990) for galactic globular clusters, Huchra et al. (1996) for the Fornax dSph globular clusters and Schroder et al. (2002) for the M 81 globular clusters. All observations were made in the Lick system. The data on M_V, V and I for the galactic GCs were taken from the catalog of Harris (1996).

4. Globular cluster metallicity and age

Metallicities for the observed GCs were calculated using the linear least-square fits of the indices versus metallicity for metallicity-sensitive line indices made by Covino et al. (1995). We obtained the mean metallicity of the cluster in DDO 78 and the mean metallicities of Galactic GCs (Table 6) by taking the error-weighted average of the metallicities predicted by the strength of five metallicity-sensitive absorption-line indices: Mgb, Fe 5270, Fe 5335, Mg_1 and Mg_2. It should be noticed that Mg_1 and Mg_2 each was assigned half weight, because these indices are tightly correlated (Burstein et al. 1984). A comparison of the indices measured by us for the core of the

Table 4. Calibration of our index measurements into the standard Lick system. Top: a comparison of the Lick indices measured with the Long-slit spectrograph UAGS (6 m telescope) with those from Worthey et al. (1994) for the observed stars. Bottom: a comparison of the twilight sky Lick indices measured with the Multi-Pupil Fiber Spectrograph of the 6 m telescope with those measured with the UAGS (see text for details). The values of atomic indices are given in Å. The values of molecular indices are given in magnitudes.

Object	Hβ	Mgb	Fe 5270	Fe5335	Mg$_1$	Mg$_2$
HD 073593 (Lick/IDS)	1.38 ± 0.22	3.08 ± 0.23	2.96 ± 0.28	2.16 ± 0.26	0.072 ± 0.007	0.183 ± 0.008
HD 073593 (UAGS)	1.10 ± 0.13	2.75 ± 0.30	2.99 ± 0.43	2.22 ± 0.33	0.064 ± 0.018	0.138 ± 0.021
HD 091739 (Lick/IDS)	3.75 ± 0.22	1.09 ± 0.23	1.35 ± 0.28	1.25 ± 0.26	0.013 ± 0.007	0.070 ± 0.008
HD 091739 (UAGS)	3.58 ± 0.11	1.13 ± 0.12	1.20 ± 0.13	0.86 ± 0.20	−0.014 ± 0.007	0.033 ± 0.008
HD 152792 (Lick/IDS)	2.02 ± 0.22	1.82 ± 0.23	0.92 ± 0.28	1.10 ± 0.26	–	0.084 ± 0.008
HD 152792 (UAGS)	2.17 ± 0.19	2.03 ± 0.13	1.57 ± 0.21	1.07 ± 0.19	0.007 ± 0.011	0.083 ± 0.013
HD 142373 (Lick/IDS)	2.26 ± 0.22	2.01 ± 0.23	0.71 ± 0.28	0.96 ± 0.26	0.007 ± 0.007	0.078 ± 0.008
HD 142373 (UAGS)	2.37 ± 0.20	1.76 ± 0.12	1.21 ± 0.20	0.92 ± 0.26	0.003 ± 0.010	0.062 ± 0.011
Twilight sky (MPFS)	1.86 ± 0.03	2.59 ± 0.05	2.04 ± 0.06	1.59 ± 0.11	0.002 ± 0.004	0.066 ± 0.002
Twilight sky (UAGS)	1.97 ± 0.04	2.52 ± 0.02	2.13 ± 0.07	1.76 ± 0.12	−0.033 ± 0.010	0.012 ± 0.006

Table 5. Calibrated indices and errors for the observed globular clusters. The values of atomic indices are given in Å. The values of molecular indices are given in magnitudes.

Object	Hβ	Mgb	Fe 5270	Fe 5335	Mg$_1$	Mg$_2$
GC in DDO 78	1.36	0.80	0.87	0.55	0.023	0.037
	±0.23	±0.27	±0.37	±0.40	±0.015	±0.018
NGC 2419	2.16	0.37	0.92	0.68	-0.024	-0.004
	±0.54	±0.49	±0.45	±0.831	±0.025	±0.030
NGC 4147	2.19	0.66	0.78	0.67	0.005	0.035
	±0.12	±0.15	±0.19	±0.098	±0.006	±0.008
Pal 1	2.17	1.79	1.56	1.40	0.029	0.097
	±0.43	±0.43	±0.52	±0.632	±0.020	±0.024
NGC 5272	2.88	1.07	1.19	0.96	0.007	0.059
	±0.08	±0.18	±0.22	±0.16	±0.008	±0.009

Table 6. Metallicity predicted by each spectral feature and the error weighted metallicity of each cluster.

Object	Mgb	Fe 5270	Fe 5335	Mg$_1$	Mg$_2$	[Fe/H]$_{our}$	[Fe/H]$_{ZW}$
GC in DDO 78	−1.60	−1.78	−1.88	−1.35	−1.79	−1.6	–
	±0.13	±0.29	±0.41	±0.30	±0.18	±0.1	
NGC 2419	−1.81	−1.73	−1.75	−2.30	−2.21	−2.08	−2.10
	±0.55	±0.83	±1.94	±0.50	±0.30	±0.24	±0.30
NGC 4147	−1.67	−1.85	−1.76	−1.71	−1.82	−1.75	−1.80
	±0.17	±0.34	±0.23	±0.13	±0.08	±0.07	± 0.26
Pal 1	−1.09	−1.21	−1.00	−1.24	−1.19	−1.17	−0.6
	±0.49	±0.94	±1.47	±0.40	±0.24	±0.21	± 0.2
NGC 5272	−1.46	−1.51	−1.46	−1.67	−1.57	−1.56	−1.66
	±0.20	±0.40	±0.38	±0.15	±0.09	±0.08	± 0.06

Milky Way GC NGC 5272 = M 3 with the corresponding values from Burstein et al. (1984) shows a good agreement. The estimates of [Fe/H] derived by us for Galactic GCs NGC 2419, NGC 4147, and M 3 agree also rather well with the catalogue values: in the last column of Table 6 the estimates from Zinn & West are given for every cluster. As for Pal 1, whose metallicity given in Table 6 has been found by Rosenberg et al. (1998a), this cluster is known to be much younger than the bulk of other Galactic globular clusters (T(Pal1) = 6–8 Gyr, Rosenberg et al. 1998b); so the calibration of metallicity-sensitive indices made by using the old globular clusters is not applicable to it. The value [Fe/H] = −1.6 ± 0.1 dex calculated in the present work
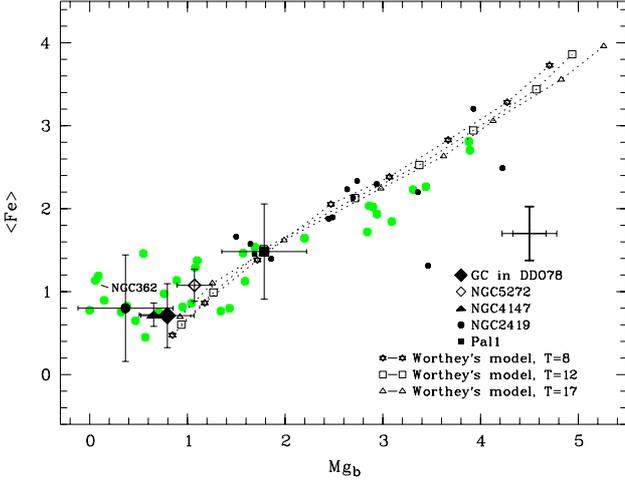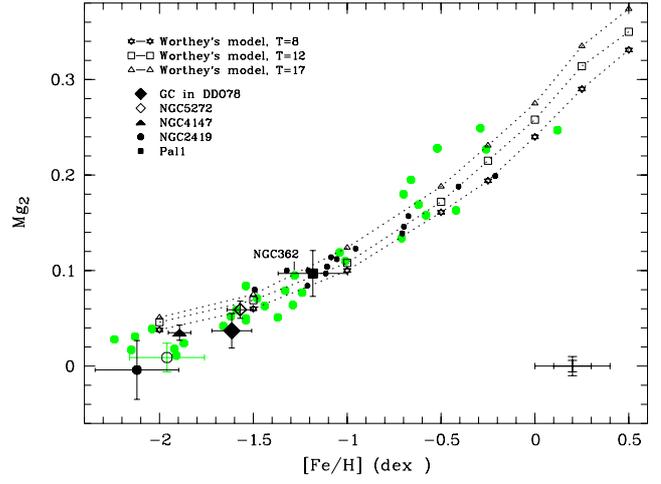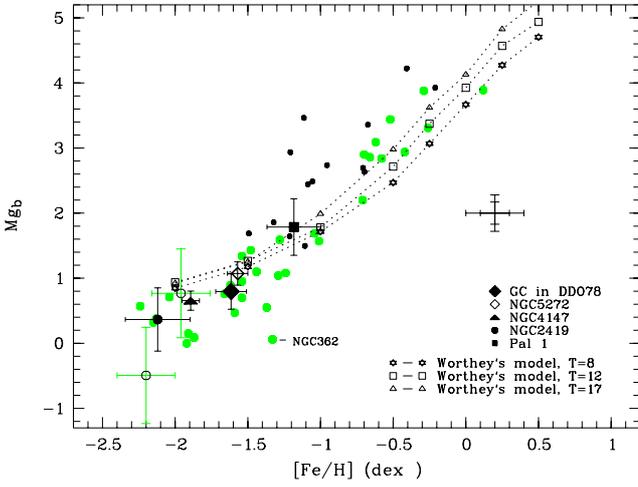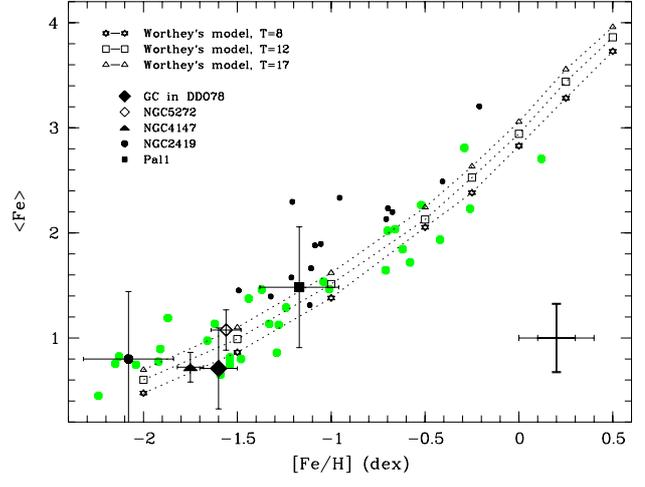
Fig.3a

Fig.3b

Fig.3c

Fig.3d

Fig. 3. $\langle Fe \rangle$ = (Fe5270 + Fe5335)/2 plotted against Mgb index (Fig. 3a); also we show [Fe/H] correlations with the metallicity-sensitive indices Mg_2 (Fig. 3b), Mgb (Fig. 3c), and $\langle Fe \rangle$ (Fig. 3d) for the observed globular clusters (signs marked on the plot), for Milky Way (grey dots), M 81 (dark small dots) and Fornax DSph globular clusters (open circles). Typical errors for the M 81 clusters are shown with the long bars; for Galactic clusters, with the short bars. The ages of Worthey's (1994) models are given in gigayears. The metallicities for Worthey's models are -2.00, -1.50, -1.00, -0.50, -0.22, 0.00, $+0.25$, $+0.50$, if one takes the signs from left to the right.

for the GC in DDO 78 does not contradict the mean metallicity of the galaxy itself derived from the red giant branch morphology by Karachentsev et al. (2000), [Fe/H] = -1.6 ± 0.3 dex.

Figure 3a shows the index $\langle Fe \rangle$ = (Fe5270 + Fe5335)/2 as a function of the index Mgb. It is evident that the GC in DDO 78 follows well Worthey's models and is similar to the galactic globular clusters in this diagram. A comparison of the metallicity-sensitive indices with the corresponding values for the Galactic GC with [Fe/H] ~ -1.6 dex shows a good agreement. In Figs. 3b–3d we plot the strengths of Mg_2, Mgb, and $\langle Fe \rangle$ as a function of [Fe/H]. The low-metallicity Galactic and M 81 GCs and GC in DDO 78 occupy generally the same positions in these figures.

We continue our analysis by plotting various indices as a function of $(V - I)$ color corrected for extinction, adopting the photometry of Karachentsev et al. (2000) for the globular cluster in DDO 78. Figures 4a–4d show $(V - I)_0$ color versus Mgb,

Mg_2, $\langle Fe \rangle$ and [Fe/H]. It is clear that the GC in DDO 78 falls rather into a group of low-metallicity Galactic GGs. However, its $(V - I)_0$ color seems to be too red.

$(V - I)_0$ colors for M 81 GCs were computed from $(B - V)$ colors derived by Schroder et al. (2002) and corrected for foreground reddening and for the mean value of internal reddening in M 81 computed by the latter authors. We used the relationship between intrinsic $(B - V)$ and $(V - I)$ colors for Milky Way GCs with the integrated spectral type F9/G0-G2 from Reed et al. (1988).

To obtain the age of the GC in DDO 78 we plot the age-sensitive index Hβ against Mgb (Fig. 5a), Mg_2 (Fig. 5b), $\langle Fe \rangle$ (Fig. 5c), and [Fe/H] (Fig. 5d). The signs are the same as in the previous figures.

Figure 5 demonstrates that the GC in DDO 78 has a too low Hβ for its weak metal absorption lines: it falls below the oldest model sequence, $T = 17$ Gyr. However, it is not a single
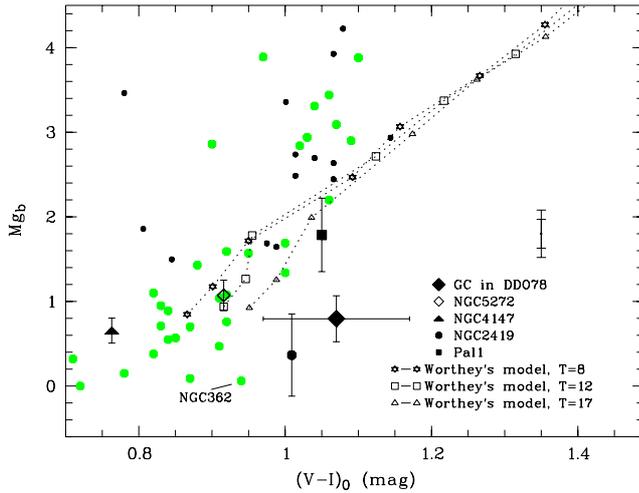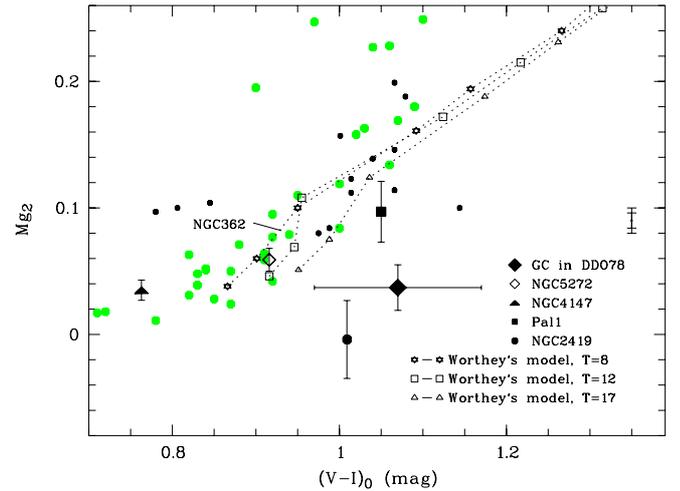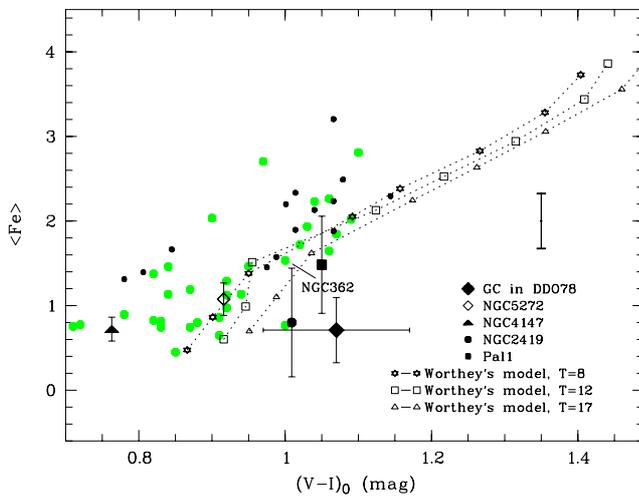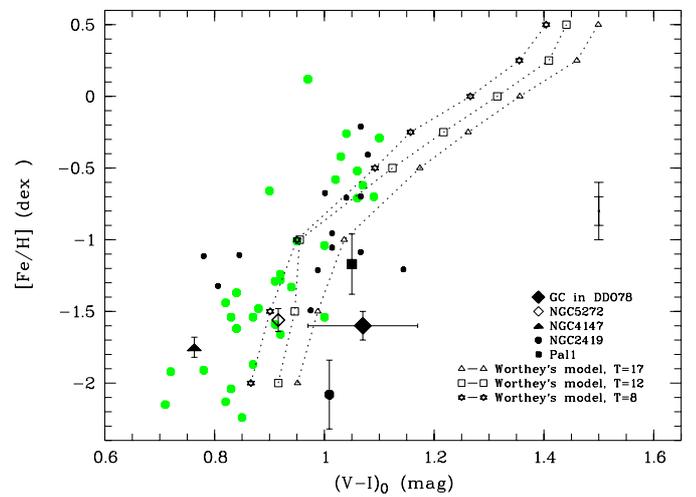
Fig.4a

Fig.4b

Fig.4c

Fig.4d

Fig. 4. Mgb index (Fig. 4a), Mg_2 (Fig. 4b), $\langle Fe \rangle$ (Fig. 4c) and [Fe/H] (Fig. 4d) plotted as a function of $(V-I)_0$ color. The symbols are the same as in the Fig. 3. $(V-I)_0$ color for GCs is taken from the catalog of Harris (1996).

outlier: the whole group of the Galactic globular clusters with red horizontal branches, mostly of intermediate metallicity, are also well below the 17-Gyr model sequence of Worthey (1994). The problem is not our finding: Covino et al. (1995), comparing their index measurements for Galactic globular clusters with the models of Buzzoni et al. (1992, 1994), which included an EMPIRICAL RED horizontal branch, have also found the same shift. They have suggested that this discrepancy results from the solar $[\alpha/Fe]$ ratio of the models: if one takes α-enhanced isochrones, the isochrone turn-off points would be redder (cooler), and the corresponding Hβ equivalent widths would be lower. Since the Galactic globular clusters are known to have [O/Fe] = +0.3 ÷ +0.5, their suggestion seemed to be the solution. However, during the last years, there were numerous attempts to improve model isochrones and evolutionary synthesis approaches to globular clusters, and none of them corrects the discrepancy in Fig. 5. Salaris & Weiss (1998) have reported their new α-enhanced isochrones, from which one can see that for the intermediate metallicity, [Fe/H] = −1.35 dex,

the α-element enhancement affects the slope of the giant branch on the C-M diagram, but leaves the main-sequence turn-off position unaffected. Maraston (1998) (see also Maraston et al. 2001) has revised the Hβ estimates by evolutionary synthesis with new isochrones and the fuel-consumption theorem application to the horizontal branch treatment, but her Hβ indices are even higher than those of Worthey (1994) and Buzzoni et al. (1992, 1994).

So, a conclusion must be made that current state-of-the-art models cannot explain some intermediate-metallicity globular clusters, namely, almost all the clusters with red horizontal branches. Under such circumstances the only reasonable way to determine the age of the GC in DDO 78 is to compare it with a Galactic globular cluster for which a detailed C-M diagram is available. The nearest neighbor of the GC in DDO 78 in Fig. 5 is the well-studied Galactic globular cluster NGC 362. While the metallicities of most globular clusters with red horizontal branches are higher than [Fe/H] = −1 dex, the metallicity of NGC 362 is only slightly higher than that of the GC
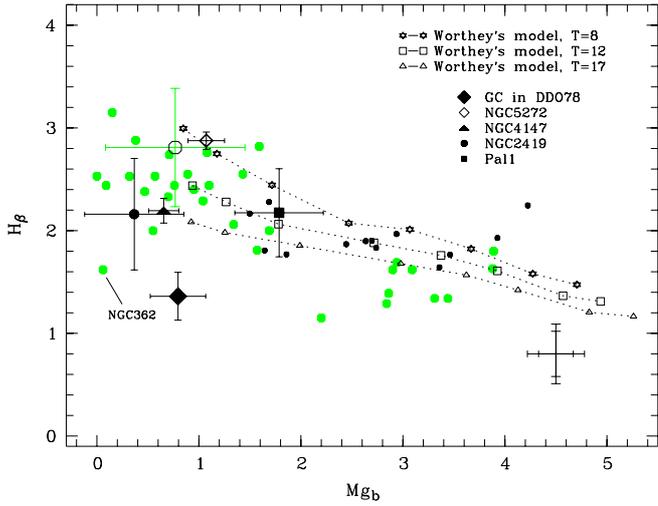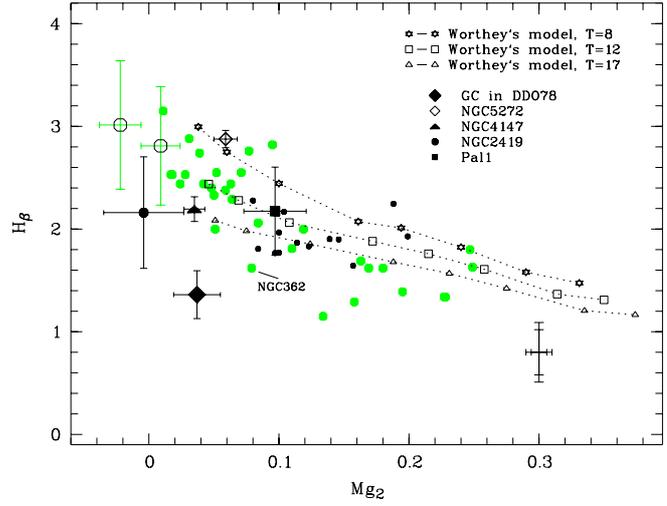
Fig.5a

Fig.5b
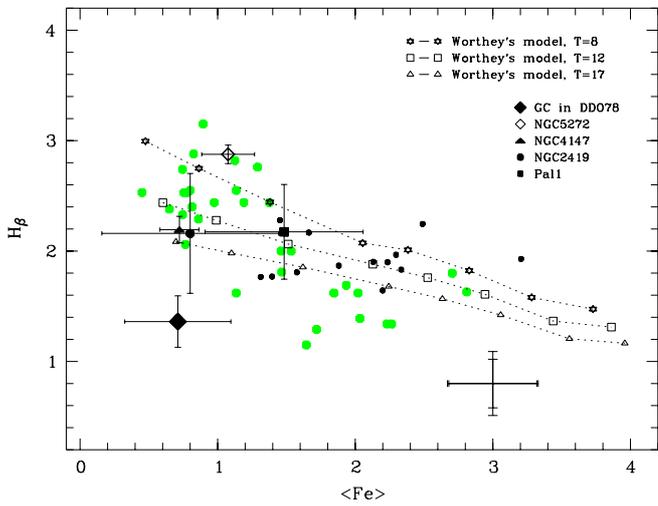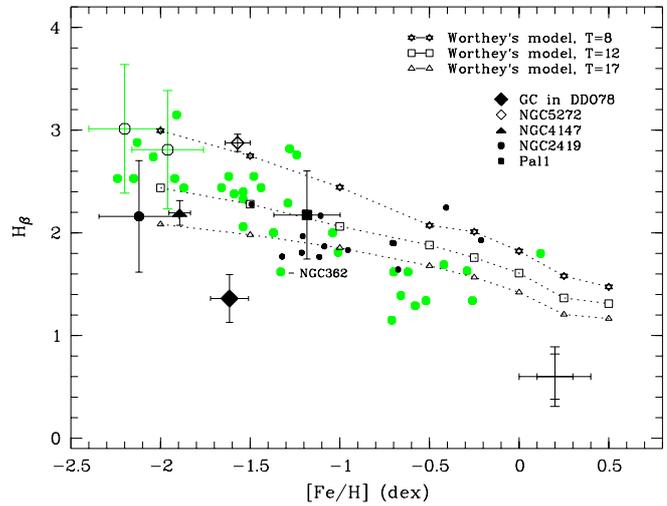

Fig.5c

Fig.5d

Fig. 5. The age-sensitive index Hβ plotted as a function of Mgb (Fig. 5a), Mg$_2$ (Fig. 5b), ⟨Fe⟩ (Fig. 5c) and [Fe/H] (Fig. 5d). The symbols are the same as in the Fig. 3.

in DDO 78, namely, its [Fe/H] = −1.33 ± 0.01 dex (Shetrone & Keane 2000), and it is a member of the classical second-parameter cluster pair NGC 288/NGC 362. These two clusters have the same metallicities, but quite different morphologies of the horizontal branches, the horizontal branch of NGC 362 being a red one. After a long discussion about the nature of the second parameter determining a morphology of the horizontal branches, a common view is established that it may be age; in particular, a careful examination of the C-M diagrams of NGC 288 and NGC 362 by Bellazzini et al. (2001) and Catelan et al. (2001) has proved that the latter cluster is younger by 1.5–2 Gyr than the former. The estimates of the absolute age of NGC 362 range from 8.7 Gyr (Salaris & Weiss 1998) and 9.9 Gyr (Carretta et al. 2000) to 11–12 Gyr (Vandenberg 2000). Since the differences of Hβ, Mg$_2$, Mgb, and ⟨Fe⟩ indices between NGC 362 and GC in DDO 78 are practically within the observational errors, we can suggest that the age of the GC in DDO 78 is also about 9–12 Gyr.

5. Discussion

According to Burgarella et al. (2001) the mean metallicity of metal-poor globular cluster systems is weakly dependent on the host galaxy's properties and is almost "universal" at [Fe/H] ∼ −1.4 ± 0.3 dex. The metallicity of the GC in DDO 78 [Fe/H] = −1.6 ± 0.1 dex agrees well with this value. There are two DSph companions of the Milky Way which contain globular clusters: Fornax and Sagittarius DSph galaxies. Fornax DSph has the absolute integral magnitude $M_V = -13.7$, and the distance from the Milky Way is 140 kpc (van den Bergh 2000). These properties are comparable to those of DDO 78, which is located at the distance of 223 kpc from M 81 (Karachentsev et al. 2002). Five Fornax DSph globular clusters have the mean metallicity [Fe/H] = −2.04 dex, essentially the same ages (| δt |< 1 Gyr) and are coeval with the old, metal-poor clusters of our Galaxy (Buonanno et al. 1998) Unfortunately, there are no measured integrated absorption indices for all Fornax

GCs in the literature. Fornax DSph GCs 3 and 5 show absorption feature strengths (Huchra et al. 1996) unlike those for the GC in DDO 78. Our cluster seems to be more metal-rich than the Fornax DSph GCs. We found only one Galactic globular cluster with measured integral absorption indices, NGC 362, which resembles the GC in DDO 78 in all properties within the errors. NGC 362 has the galactocentric radius $R_{gc} = 9.2$ kpc, the integral absolute visual magnitude $M_V = -8.4$ and resembles in its properties some intermediate-metallicity clusters with $R_{gc} > 8$ kpc, NGC 1851, NGC 1261, NGC 2808 (Rosenberg et al. 1999). These clusters are younger by $\sim$2 Gyr than the metal-poor halo GCs and are associated with so-called "streams" that may be relics of ancient Milky Way satellites that had masses typical of a dwarf galaxy.

The M 81 group of galaxies has a structure similar to the LG (Karachentsev et al. 2000). The subgroups around the Sb type galaxies, the Milky Way and M 31, have a spatial separation of $\sim$1 Mpc and approach each other at a velocity of $\sim$130 km s^{-1}. Such a situation resembles the M 81/NGC 2403 complex. But there are some differences between the two groups. The core members of the M 81 group, M 81, M 82, NGC 3077 and NGC 2976, are known to be closely interacting from the aperture synthesis maps of the 21 cm HI emission (Yun et al. 1994; Boyce et al. 2001). The dwarf spheroidal galaxies are distributed around M 81 asymmetrically (Karachentsev et al. 2001). With respect to the group centroid (located between M 81 and M 82) all DSphs are concentrated in one quadrant. Jonson et al. (1997) reported the discovery of the high-excitation HII region in K 61, the brightest DSph galaxy of the M 81 group and the closest companion to M 81. They found the metallicity of the HII region, Z, between 0.001 and 0.008, and the age between 2 and 5.2 Myr. The properties of DSph galaxies appear to be correlated with the galaxy mass and with environment. Does the tidal interaction between the brightest M 81 group galaxies influence the distribution and star formation histories of DSphs? Accurate numerical simulations are needed.

References

Afanasiev, V. L., Burenkov, A. N., Vlasyuk, V. V., & Drabek, S. V. 1995, SAO RAS Internal Rep., 234
Afanasiev, V. L., & Sil'chenko, O. K. 2002, AJ, 124, 706
Barbier-Brossat, M., & Figon, P. 2000, A&AS, 142, 217
Bellazzini, M., Pecci, F. F., Ferraro, F. R., et al. 2001, AJ, 122, 2569
Bohlin, R. C. 1996, AJ, 111, 1743
Boyce, P. J., Minchin, R. F., Kilborn, V. A., et al. 2001, ApJ, 560, L127
Brodie, J. P., & Huchra, J. P. 1990, ApJ, 362, 503
Buonanno, R., Corsi, C. E., Zinn, R., et al. 1998, ApJ, 501, L33
Burgarella, D., Kissler-Patig, M., & Buat, V. 2001, AJ, 121, 2647
Burstein, D., Faber, S. M., Gaskell, C. M., & Krumm, N. 1984, ApJ, 287, 586
Buzzoni, A., Gariboldi, G., & Mantegazza, L. 1992, AJ, 103, 1814
Buzzoni, A., Mantegazza, L., & Gariboldi, G. 1994, AJ, 107, 513
Cardiel, N., Gorgas, J., Cenarro, J., & Gonzalez, J. J. 1998, A&AS, 127, 597
Carretta, E., Gratton, R. G., Clementini, G., & Fusi Pecci, F. 2000, ApJ, 533, 215
Catelan, M., Bellazzini, M., Landsman, W. B., et al. 2001, AJ, 122, 3171
Cohen, J. G., Blakeslee, J. P., & Ryzhov, A. 1998, ApJ, 496, 808
Covino, S., Galletti, S., & Pasinetti, L. E. 1995, A&A, 303, 79
Faber, S. M., Burstein, D., & Dressler, A. 1977, AJ, 82, 941
Fisher, J. R., & Tully, R. B. 1981, ApJS, 47, 139
Grebel, E. K. 2000, 33rd ESLAB Symp. on Star Formation from the Small to the Large Scale, SP-445, ed. F. Favata, A. A. Kaas, & A. Wilson (Noordwijk: ESA), 87
Harbeck, D., Grebel, E., Holtzman, J., et al. 2002, AJ, 122, 3092
Harris, W. E. 1996, AJ, 112, 1487
Huchra, J. P., Brodie, J. P., Caldwell, N., Christian, C., & Schommer, R. 1996, ApJS, 102, 29
Johnson, R. A., Lawrence, A., Terlevich, R., & Carter, D. 1997, MNRAS, 287, 333
Karachentseva, V. E., Karachentsev, I. D., Richter, G. M., von Berlepsh, R., & Fritze, K. 1987, Astron. Nachr., 308, 247
Karachentsev, I. D., Karachentseva, V. E., Dolphin, A. E., et al. 2000, A&A, 363, 117
Karachentsev, I. D., Dolphin, A. E., Geisler, D., et al. 2002a, A&A, 383, 125
Maraston, C. 1998, MNRAS, 300, 872
Maraston, C., Greggio, L., & Thomas, D. 2001, Ap&SS, 276, 893
Reed, B. C., Hesser, J. E., & Shawl, S. J. 1988, PASP, 100, 545
Rosenberg, A., Piotto, G., Saviane, I., Aparicio, A., & Gratton, R. 1998a, AJ, 115, 658
Rosenberg, A., Saviane, I., Piotto, G., Aparicio, A., & Zaggia, S. R. 1998b, AJ, 115, 648
Rosenberg, A., Saviane, I., Piotto, G., & Aparicio, A. 1999, AJ, 118, 2306
Salaris, M., & Weiss, A. 1998, A&A, 335, 943
Schroder, L. L., Brodie, J. P., Kissler-Patig, M., Huchra, J. P., & Phillips, A. C. 2002, AJ, 123, 2473
Sharina, M. E., Karachentsev, I. D., & Burenkov, A. N. 2001, A&A, 380, 435
Shetrone, M. D., & Keane, M. J. 2000, AJ, 119, 840
Smith, E. O., Rich, M., & Neill, J., AJ, 115, 2369
Stetson, P. B., Hesser, J. E., & Smecker-Hane, T. A. 1998, PASP, 110, 533
Trager, S. C., Worthey, G., Faber, S. M., Burstein, D., & Gonzalez, J. J. 1998, ApJS, 116, 1
Vandenberg, D. A. 2000, ApJS, 129, 315
van den Bergh, S. 2000, The galaxies of the Local Group (Cambridge Univ. Press)
van Driel, W., Kraan-Korteweg, R. C., Binggeli, B., & Huchtmeier, W. K. 1998, A&AS, 127, 397
Worthey, G. 1994, ApJS, 95, 107
Worthey, G, Faber, S. M., Gonzalez, J. J., & Burstein, D. 1994, ApJS, 94, 687
Yun, M. S., Ho, P. T. P., & Lo, K. Y. 1994, Nature, 372, 530
Zinn, R., & West, M. J. 1984, ApJS, 55, 45